Changes in the Concentration of Mesospheric O_3 and OH During a Highly Relativistic Electron Precipitation Event

R. A. Goldberg[1], C. H. Jackman[2], D. N. Baker[1], and F. A. Herrero[1]

NASA/Goddard Space Flight Center, Greenbelt, Maryland

Highly relativistic electron precipitation events (HREs) can provide a major source of energy affecting ionization levels and minor constituents in the mesosphere. Based on satellite data, these events are most pronounced during the minimum of the solar sunspot cycle, increasing in intensity, spectral hardness and frequency of occurrence as solar activity declines. Furthermore, although the precipitating flux is modulated diurnally in local time, the noontime maximum is very broad, exceeding several hours. Since such events can be sustained up to several days, their integrated effect in the mesosphere can dominate over those of other external sources such as relativistic electron precipitation events (REPs) and auroral precipitation. In this work, the effects of HRE relativistic electrons on the neutral minor constituents OH and O_3 are modeled during a modest HRE, to estimate their anticipated impact on mesospheric heating and dynamics. The data to be discussed and analyzed were obtained by rocket at Poker Flat, Alaska on May 13, 1990 during an HRE observed at midday near the peak of the sunspot cycle. Solid state detectors were used to measure the electron fluxes and their energy spectra. An x-ray scintillator was included to measure bremsstrahlung x-rays produced by energetic electrons impacting the upper atmosphere; however, these were found to make a negligible contribution to the energy deposition during this particular HRE event. Hence, the energy deposition produced by the highly relativistic electrons dominated within the mesosphere and was used exclusively to infer changes in the middle atmospheric minor constituent abundances. By employing a two-dimensional photochemical model developed for this region at Goddard Space Fight Center, it has been found that for this event, peak modifications in the neutral minor species occurred near 80 km. A maximum enhancement for OH was calculated to be over 40% at the latitude of the launch site, which in turn induced a maximum depletion of O_3 in excess of 30%. Since this particular HRE occurred near solar maximum, it was of modest intensity and spectral hardness, parameters which could grow significantly as solar minimum is approached. Estimates of mesospheric OH enhancement and O_3 depletion have also been made for more intense HRE events, as might be expected during the declining phase of the solar cycle. The findings imply that the energy deposition from highly relativistic electrons during more intense HREs could modulate the concentration of important minor species within the mesosphere to much higher levels than estimated for the observed HRE. By causing O_3 destruction, the electron precipitation can also modify the penetration depth of solar UV radiation, which may affect thermal properties of the mesosphere to depths approaching 60 km.

1) Laboratory for Extraterrestrial Physics
2) Laboratory for Atmospheres

The Upper Mesosphere and Lower Thermosphere:
A Review of Experiment and Theory
Geophysical Monograph 87

Published in 1995 by the American Geophysical Union

INTRODUCTION

Highly relativistic electron precipitation events (HREs) may provide the major source of ionization energy from precipitating electrons affecting mesospheric constituents. Based on satellite data, these events are most pronounced during the declining phase of the solar cycle, increasing in intensity, spectral hardness, and frequency of occurrence as the solar cycle reaches minimum [e.g., *Baker et al.*, 1987, 1993]. Since such events can be sustained up to several days, their integrated effect in the mesosphere can potentially dominate other sources of energy input such as relativistic electron precipitation events (REPs) and auroral precipitation events (APEs). Here, the effects of an HRE on mesospheric neutral minor constituents such as ozone (O_3) during a measured HRE are modeled, to demonstrate its impact on these constituents.

It has been known for some time that solar protons impact the middle atmosphere and affect its neutral and electrodynamic structure. Rocket measurements by Weeks et al. [1972] during the large solar proton event (SPE) of November, 1969 were used by Swider and Keneshea [1973] in a model calculation to demonstrate that solar proton events (SPEs) could modify mesospheric HO_X, O_3, and other minor constituents. For the great SPE in August, 1972, Heath et al. [1977] showed a remarkable depletion in stratospheric O_3 by measuring solar backscattered ultraviolet radiation with the SBUV instrument aboard Nimbus IV. This O_3 depletion required several weeks for recovery following the event [*Jackman and McPeters*, 1987]. Thomas et al., [1983], Solomon et al. [1983], McPeters and Jackman [1985], and Jackman and McPeters [1985] have also investigated and/or modeled significant middle atmospheric O_3 depletions caused by several other SPEs of varying magnitudes. More recently, Johnson and Luhmann [1993] have shown evidence for SPE modulation of mesospheric dynamical structure, comparing Poker Flat MST Radar data with SPE occurrences during the early 1980s. Finally from the electrodynamic viewpoint, ionization enhancements from SPEs are sufficiently intense and well defined to have caused a renaming of SPEs as polar cap absorption events (PCA), in response to the major ionization effects caused by SPEs at high magnetic latitudes.

REPs and APEs are relatively short-lived compared to SPEs. Since REPs and APEs are much less intense and do not usually penetrate as deeply into the atmosphere, they are more likely to have their maximum effect in the mesosphere; i.e., maximum electron energies between 0.5 and 1.0 MeV usually restrict energy deposition by REPs and APEs to atmospheric altitudes above 60 km [*Goldberg et al.*, 1984; *Jackman*, 1991]. Thorne [1980] has argued that REP events might have as significant an impact on the middle atmosphere as SPEs, because of their much higher frequency of occurrence. However, his definition of REPs may have been expanded to include all relativistic electron precipitations, including those associated with auroral geomagnetic disturbances and possibly HREs, which are usually characterized by a harder energy spectrum.

HREs represent the most intense and spectrally hard electron events observed to date. Details of these events as observed at geosynchronous satellite altitudes can be found in Baker et al. [1979, 1986]. From comparisons with lower altitude satellites [*Imhof et al.*, 1991], and from the rocket study to be evaluated here, it is apparent that a significant fraction of the outer zone (high altitude) electrons associated with an HRE reach the middle atmosphere [*Herrero et al.*, 1991; *Baker et al.*, 1993] and strongly influence the electrodynamics of that region [*Goldberg et al.*, 1994]. Since HREs can sustain their activity for several days (albeit with a diurnal variability having a wide local noontime maximum of several hours) and recur over several solar rotations, and since they may cover a broader region in longitude and latitude than the auroral zone, their impact on the middle atmosphere should be large.

This paper considers an HRE that occurred in May 1990 as reported earlier [*Herrero et al.*, 1991; *Baker et al.*, 1993; *Goldberg et al.*, 1994]. It is concerned with the influence that the HRE electrons had on the minor constituents OH and O_3 within the mesosphere, the region where most of the HRE electron energy from this event was absorbed. It is based on results obtained from rocket payloads launched during the event from Poker Flat Research Range, Alaska. The event studied was found to be relatively modest, which is to be expected immediately following the maximum of the solar cycle. Nonetheless, the results from a GSFC two-dimensional photochemical model imply that the modest fluxes observed in this event were capable of modifying the OH and O_3 concentrations in the mesosphere by a measurable amount.

EXPERIMENT DESCRIPTION

General Considerations

In May of 1990 multiple payloads were launched in a rocket experiment to measure the relativistic electron fluxes reaching the middle atmosphere during an HRE, and to investigate the influence of HREs on the electrodynamical and neutral properties of the middle atmosphere. Since the relativistic electron precipitation events are thought to be increasingly frequent and more intense following the solar maximum period, it was the goal of the May 1990

Table 1. Characteristics of Taurus-Orion flight trajectories.

ROCKET		LAUNCH		APOGEE		
Number	Type	Date	Time (UT)	Altitude (km)	Time (TSL, sec)	Horizontal Range (km)
33.059	Taurus Orion	13 May 90	2129:02	130.4	184	44.0
33.060	Taurus Orion	14 May 90	2026:00	127.9	182	45.5

experiment to first measure the intensity and energy spectrum of these relativistic electrons in the middle atmosphere for a modest event near solar maximum. Poker Flat, Alaska was selected because it lies at the equatorward edge of the auroral zone, where representative components of precipitating electron showers are normally expected to occur, and where there is the opportunity to coordinate measurements with those from a ground station and from a geostationary spacecraft on approximately the same magnetic field line.

The linear prediction filter of Baker et al. [1990] was used to anticipate when relativistic electrons should be at their maximum levels. This technique utilizes ground-based geomagnetic indices as input time series and gives a reasonable level of confidence for predicting enhancements months in advance of their occurrence. Real-time data from operational spacecraft in synchronous orbit were also available to help judge the specific time when the rocket launches should occur. These data were accessed via the NASA/SPAN computer network and were resident on computers at the Los Alamos National Laboratory and the NOAA Space Environment Laboratory.

Two Taurus-Orion rockets and one Orion rocket were launched into an HRE event of modest intensity near local noon on May 13-14, 1990, when outer zone trapped electrons were locally at peak diurnal intensity. Apogee for each Taurus-Orion rocket trajectory was about 130 km, providing full coverage of the mesosphere and part of the lower thermosphere. Each Taurus-Orion payload contained a mix of solid state and x-ray detectors to measure the energetic radiation at and below about 130 km altitude, and an assortment of plasma probes and an electric field symmetric boom array to measure middle atmospheric electrodynamic response to the impinging radiation. In addition, Taurus-Orion 33.059, launched on May 13, 1990, was immediately followed by an Orion payload (30.035), containing assorted instrumentation to measure the electrodynamic properties of the middle atmosphere in more detail than on the Taurus-Orion. This work makes use of the flux measurements obtained on 33.059 and 33.060 to evaluate the expected perturbations of the measured HRE on OH and O_3. The electrodynamic properties of the atmosphere obtained from this study can be found in Goldberg et al. [1994] and will not be discussed further in this paper. Table 1 lists the Taurus-Orion rocket flights with their relevant specifications.

Critical Instrument Descriptions

Most instruments flown on the Taurus-Orion and Orion payloads have been described in elsewhere [*Herrero et al.*, 1991; *Goldberg et al.*, 1994]. The electron spectrometers and the x-ray scintillator are briefly described here, because of their prime use in measuring the electron energy flux. Each Taurus-Orion payload included two silicon (Li-drifted) solid state electron spectrometers to detect low energy electrons (0.09-1.0 MeV, 12 differential channels) and high energy electrons (0.4 to 3.8 MeV, 8 differential channels), respectively. In addition, each payload carried an x-ray NaI scintillator detector to measure bremsstrahlung x-rays and electrons above 120 keV. Each scintillator was fitted with a 125 micron Be window and optically mounted to a ruggedized photo multiplier [cf. *Goldberg et al.*, 1984 for a detailed description). Electronic sampling of the pulse amplitudes permitted sampling in the integral spectral ranges >5, >10, >20, >40, and >80 keV. These detectors were also sensitive to charged particles that can penetrate the Be window, which has a threshold for electrons near 120 keV.

During each Taurus-Orion flight, the payload was despun to approximately 1.3 Hz and then oriented at 45° to the Earth's magnetic field with a magnetic attitude control system. This permitted the solid state and x-ray detectors to sweep in look angle from 0° to 90° magnetic pitch angle during each revolution of the payload, since they were

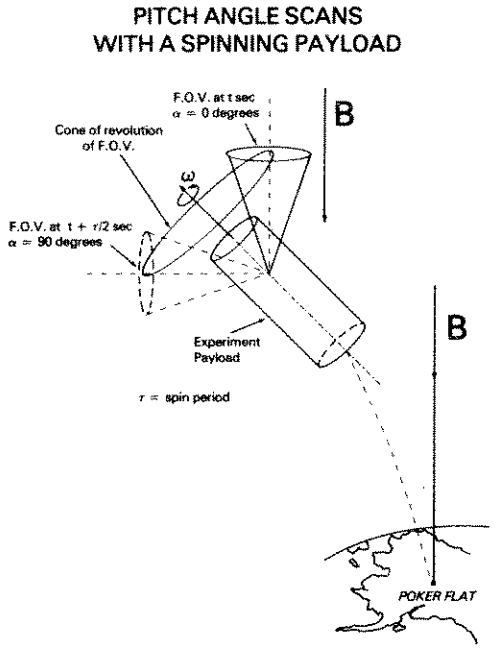

Fig. 1. Schematic view of payload geometry demonstrating how a 0-90° pitch angle sweep for spectrometers and scintillator detectors is induced by payload spin.

mounted at 45° to the spin axis. A schematic diagram depicting this function is illustrated in Figure 1. Although the fields of view for the x-ray and low energy electron detectors were large (~30° half angle), the instruments still provided useful information concerning the pitch angle distribution of impacting electrons. For the high energy electron spectrometer, the field of view was only 13.5° half angle, thereby providing higher instrumental pitch angle resolution.

DATA ANALYSIS AND RESULTS

Figure 2 depicts the count rates measured by three representative channels on each electron spectrometer during the flight of 33.059. The upper panel (a) refers to the low energy spectrometer, the lower panel (b) to the high energy spectrometer. Also shown are the trajectory of the flight and magnetic pitch attitude (Fig. 2a). The latter shows that the payload stabilized near 115 sec (~105 km) into the flight. Of note are the wide burst region encompassing "1", the narrow burst region "2", and the more nominal steady region "3". From the energy spectra measured during each of these periods, we have been able to calculate the energy deposition within the middle atmosphere produced by the measured flux.

A detailed description of the energy deposition analysis has been provided in Goldberg et al. [1984] and specifically for this flight in Goldberg et al. [1994]. Briefly, the count rates from each channel are combined to produce an exponential integral spectrum of the form:

$$J(>E) = J_0 \int_E^\infty e^{-E/E_0} dE \qquad (1)$$

where J_0 is the flux at energy $E = 0$, and E_0 is folding energy. Figure 3 provides a sample of these spectra obtained during period "3" between 230 and 231 seconds into the flight. The vertical bars on each point represent the one-sigma range for the statistical sampling rate. The upper and lower panels depict spectra obtained by the low and high energy spectrometers, respectively. The curves labeled A, B, C, and D represent least squares fits to the measured points to the left and right of each breakpoint, which appear at about 350 keV (upper) and 1700 keV (lower). The values for J_0 and E_0 for each linear segment are displayed in the upper right hand corner of each panel. From this plot we observe that the total spectrum can be described with three linear components having breakpoints near 0.35 and 1.7 MeV, since curves B and C are overlapping regions and roughly equivalent. Additional plots for events "1" and "2"

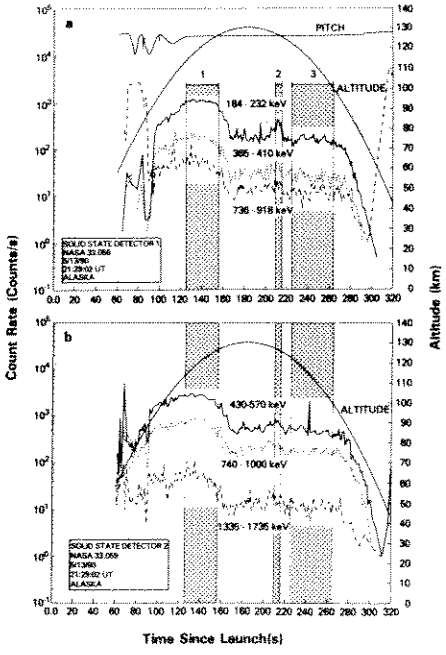

Fig. 2. Compressed view of counting rates (33.059) for three select channels on the low energy (top panel) and high energy (bottom panel) spectrometers. Payload pitch attitude (arbitrary units) and trajectory are also provided.

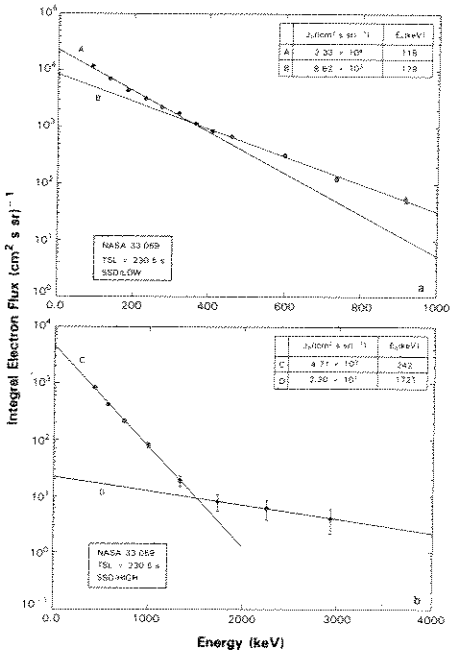

Fig. 3. Sample spectra for non-burst period "3" for 230-231 sec TSL on 33.059. Spectra for the low (top) and high (bottom) energy spectrometers are provided. The tables (upper right) give values of E_0 and J_0 for segments A and B (low energy) and C and D (high energy).

during the 33.059 flight show similar features but with increased fluxes, particularly at the lower energies. Corresponding plots were made for 33.060, but in this case from energy spectrum values averaged over the entire flight above approximately 105 km (110-260 seconds into the flight), since the electron flux at all measured energies was nearly uniform and without bursts during this period. Finally, it has been shown in Goldberg et al. [1994] that the pitch angle distribution in most cases was nearly constant; hence the flux was treated as isotropic when calculating the energy deposition.

Figure 4 shows the energy deposition profiles for the three periods "1", "2", and "3" during the 33.059 flight on May 13, 1990, and for the period in which the 33.060 payload was above 105 km on May 14, 1990, as determined from the energy deposition model of Jackman described in the Appendix of Goldberg et al. [1984]. These profiles were determined exclusively from the electron spectrometers since the contribution from bremsstrahlung x-rays was found to be negligible [*Goldberg et al.*, 1994]. This finding is unique, since x-rays have always been observed in significant quantity during auroral precipitation and REPs [e.g., *Goldberg et al.*, 1984; *Goldberg et al.*, 1990]. Also shown is the anticipated cosmic ray contribution adjusted for site location and phase of the sunspot cycle [*Nicolet*, 1975]. The peak near 80 km is probably artificially produced by cutting off the electron spectrum near 90 keV, which is the threshold for each of the low energy electron spectrometers. For example, if the sample spectrum shown in Figure 3 was extrapolated to lower energies assuming the slope remained unchanged, one would expect to see the ion-pair production rates continue to grow above 80 km as noted in Goldberg et al. [1984]. Alternatively, the near absence of low energy (5-80 keV) x-rays may signify an electron energy spectrum which decays rapidly below the 90 keV threshold of the solid state detector, thereby providing validation for that portion of the curves as shown in Figure 4 above 80 km.

From Figure 4, it is evident that the non-burst periods for 33.059 and 33.060 are similar in shape, with 33.059 exhibiting a more intense and somewhat spectrally harder electron flux. The latter can be seen through the greater depth of penetration for the 33.059 period "3" profile. Burst "2" during 33.059 shows an enhancement of flux above the non-burst periods, but mainly at the lower energies (higher altitudes). Finally, burst period "1" shows an enhancement above all other periods at all energies, but with the strongest enhancement above 60 km (below about 1 MeV). Hence, the event appears to be more intense and variable during the

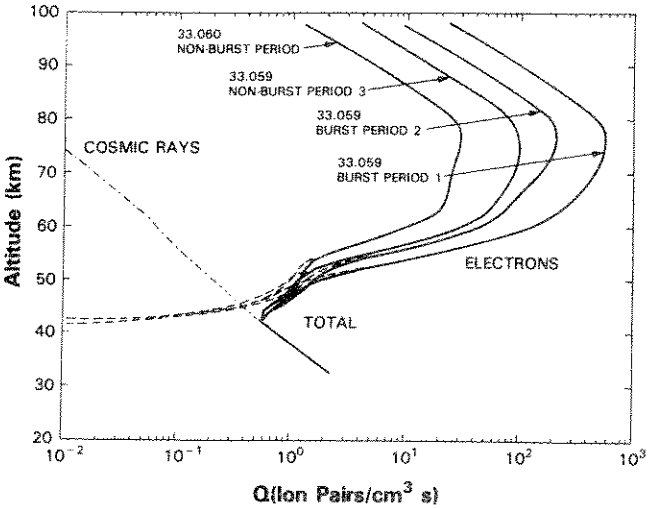

Fig. 4. Energy deposition profiles in terms of ion pair production rate caused by measured electrons. Shown are periods "1", "2", and "3" during the flight of 33.059 and the value during 33.060. Also included is the calculated effect from cosmic rays corrected for latitude and time of solar cycle. Maxima near 80 km are probably caused by limiting the electron spectrum to values above 90 keV, which is the low energy spectrometer threshold value.

flight of 33.059 on May 13, 1990, with the sample measured on May 14 representing a period during the decay of the HRE. In spite of the modest character of this HRE, these energy deposition profiles, particularly burst "1", match or exceed values measured by us during all previous aurorally active or REP events. The energy deposition profiles shown here have been used to calculate the OH and O_3 modulations discussed in the next section.

MODELING RESULTS

A NASA 2-D photochemical model has been used to calculate the mesospheric OH enhancement and O_3 depletion anticipated for this event from two of the energy deposition curves presented in Figure 4. This model is described in detail by Douglass et al. [1989] and Jackman et al. [1990]. Briefly, it employs a latitudinal range from 85°N to 85°S in 10° increments, and an altitude range from 1000 to 0.0024 mbar (0 to about 90 km) with approximately a two km resolution. Around 50 species are considered including O_x, NO_x, HO_y, Cl_y, and Br_y. The 130 chemical reactions included are as specified in JPL 90-1 [*De More et al.*, 1990]. Well known chemical-family approximations are used to reduce the number of transported species in the model.

Twenty two (22) species or families (O_x, NO_y, Cl_y, and Br_y) are transported in the model simulations used here. These include O_x (O_3, $O(^1D)$, $O(^3P)$), NO_y (N, NO, NO_2, NO_3, HO_2NO_2, N_2O_5, $ClONO_2$, but not including HNO_3), Cl_y (Cl, ClO, HOCl, HCl, $ClONO_2$), Br_y (Br, BrO, HBr, $BrONO_2$), HNO_3, N_2O, CH_4, H_2, CO, CH_3OOH, $CFCl_3$, CF_2Cl_2, CH_3Cl, CCl_4, CH_3CCl_3, CH_3Br, $CHClF_2$, $C_2Cl_3F_3$, $C_2Cl_2F_4$, C_2ClF_5, $CBrClF_2$, and $CBrF_3$. The HO_x (H, OH, HO_2) species, H_2O_2, and the hydrocarbons CH_3, CH_3O, CH_3O_2, CH_2O, and CHO are calculated using photochemical equilibrium assumptions. The CO_2 mixing ratio is set at 330 ppmv and the H_2O distribution is fixed using LIMS measurements and other model calculations [cf. *Jackman et al.*, 1987]. Ground boundary conditions for the trace gases are taken from WMO [1992, Table 8-6b], for the 1990 steady state. The residual circulation and diffusion specification is the Dynamics A formulation described in Jackman et al. [1991].

HO_x is the primary species family affecting the loss of ozone during particle precipitation events within the mesosphere. The HO_x constituents are produced by complicated ion chemistry resulting from the production of ion pairs. Each ion pair results in the formation of two HO_x species up to an altitude of approximately 70 km. Above 70 km, the HO_x species produced per ion pair depend quite strongly on the ionization rate and the duration of the particle precipitation event [*Solomon et al.*, 1981]. The 2-D model employed here does not develop the ion chemistry internally. Instead, it uses the computations of HO_x per ion pair as provided in Solomon et al. [1981, Figure 2]. HO_x enhancements can lead to O_3 depletion through several catalytic processes; these are dominated by the following catalytic process above 60 km altitude [*Jackman and McPeters*, 1987]:

$$H + O_3 \rightarrow OH + O_2 \quad (2)$$

$$OH + O \rightarrow H + O_2. \quad (3)$$

The H atom, destroyed in reaction (2), is regenerated in reaction (3) and can continue cycling through reactions (2) and (3) until either H or OH reacts with another constituent in the mesosphere. The net of reactions (2) and (3) causes O_3 and O to transform into $2O_2$.

The NASA 2-dimensional model was originally developed for use in multi-year simulations. As a result, many of the parameters are restricted to temporal variations with a minimum resolution of one day. Since HREs have a time scale of several days, but with a diurnal variability, it was necessary to use average daily values for various parameters such as the ion-pair production rate (energy deposition, Figure 4) instead of tracking it or modeling it on a smaller time-step basis. In order to use this model, it is therefore assumed that cumulative effects are considered to reach an equilibrium value within one day, which seems reasonable based on the time constants of the various processes occurring in the region of interest. Furthermore, many of the

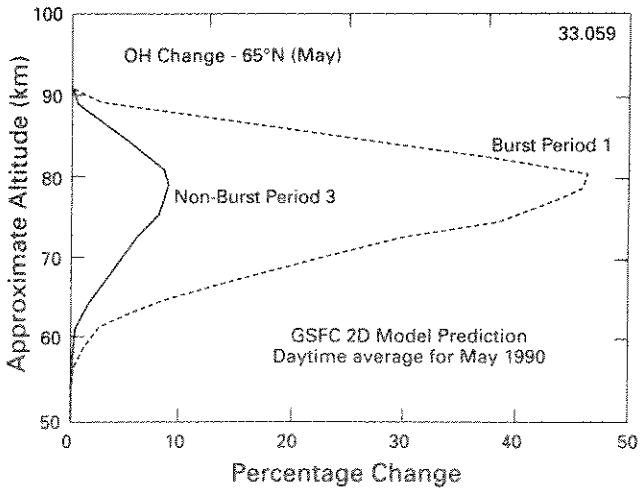

Fig. 5. The GSFC 2-D model prediction for the percent change of the OH mesospheric vertical profile at Poker Flat, Alaska (65°N) in May following bombardment by relativistic electrons with an intensity and spectral distribution equivalent to burst period "1" and non-burst period "3" in the measured HRE.

parameters are highly latitude dependent because of the rapidly changing length of day with latitude except at equinox; hence this work models the effects of the measured radiation specifically at the latitude of Poker Flat Research Range (65.1°N, 147.5°W, magnetic L = 5.5) on the date of the launch.

The four curves presented in Figure 4 all have a similar shape, with the energy deposition exhibiting a monotonic decay at all altitudes between the 33.059 burst "1" and the profile obtained from 33.060. The results obtained from the 2-D photochemical model discussed in this section concentrate on two of the four periods, viz. periods "1" and "3". Figure 5 displays the vertical profile for percentage change in OH at the Poker Flat site, assuming daytime average conditions on the date of the 33.059 launch. Figure 6 shows the resulting profile for O_3. These parameters have been calculated for the two periods assuming a one day steady source. This appears reasonable since the model approaches an equilibrium value within a few hours, which is the daily half width of the event maximum about noon. Hence, the model predicts that for a daytime average for May 1990 under burst "1" conditions, the OH would have increased by over 40% near 80 km, leading to a depletion of O_3 in excess of 30% within the same region.

The HRE and more common natural sources of HO_x compete to drive the atmospheric abundance of HO_x constituents at different times. The model background H_2O is crucial to determination of an HRE influence on the atmosphere. We have employed the H_2O climatology of Remsberg et al. [1989] for the spring-Northern Hemisphere at mid-latitudes in our 2-D model simulations. Table 2 provides the H_2O concentration profile used in our 2-D model above 0.23 mb (59 km). Since the most common natural sources of HO_x are dependent on sunlight, either from photolysis of H_2O or the reaction of $O(^1D)$ with H_2O, and since for our simulation, the HRE source of HO_x is assumed to be independent of solar zenith angle, it follows that an HRE event should have its maximum effect at the maximum solar zenith angles within its range of occurrence [e.g. see *Solomon et al.*, 1983; *Jackman and McPeters*, 1985).

Table 2. H_2O mixing ratios used in our simulations with the NASA/GSFC 2D model.

Altitude (mbar)	Altitude (km)	H_2O mixing ratio (ppmv)
0.23	59	6.0
0.17	61	6.0
0.13	63	5.2
0.098	65	5.0
0.074	67	4.3
0.056	69	3.8
0.042	71	3.2
0.031	73	2.7
0.024	75	2.1
0.018	77	1.9
0.013	79	1.7
0.010	81	1.5
0.0076	83	1.3
0.0057	85	1.1
0.0043	87	0.92
0.0032	89	0.78
0.0024	91	0.64

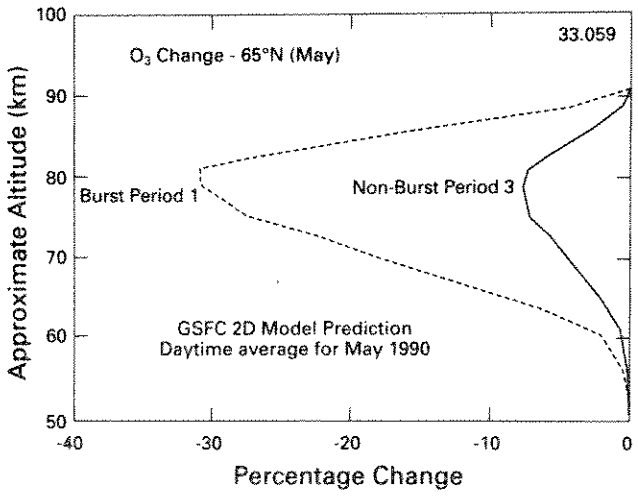

Fig. 6. The vertical profile for the percent change of O_3 under the same conditions as Figure 5.

DISCUSSION AND CONCLUSIONS

For the HRE under consideration here, Herrero et al. [1991] demonstrated that a significant portion of the relativistic electron flux observed at geosynchronous altitude reaches the middle atmosphere. Baker et al. [1993] expanded that concept and discussed the HRE effects on the stratosphere. More recently, Goldberg et al. [1994] have demonstrated the electrodynamic effects of the relativistic electron flux from this HRE on the middle atmosphere through comparisons with simultaneous measurements of electrical conductivity and related parameters. This study has considered the HRE as an energy source, and evaluated its impact on trace constituents OH and O_3 using the GSFC 2-D photochemical model. It is found that even a modest HRE of the magnitude observed and discussed here can enhance OH several percent leading to an associated depletion in O_3. For more intense HREs, as are anticipated further into the solar cycle decline, these effects could be much higher.

Since HREs are more intense than REPs and APEs and can continue for several days, their integrated effect on mesospheric ionization and minor constituents is probably much greater than that of REPs and APEs. For the relatively weak event measured during this experiment, the calculated decrease of O_3 was about 30% for daytime average conditions, but could reach much higher values near twilight. For more intense events, larger depletions of O_3 would be expected. Such depletions in O_3 would reduce the absorption of UV within the mesosphere, thereby allowing the UV radiation to penetrate to lower altitudes, leading to possible modifications of the temperature, chemistry and dynamics of the region.

Acknowledgments. We thank Neil Armour, Roy Hagemeyer, Bill Davis, Benjamin Harris, Floyd Hunsaker, and Paul Rozmarynowski for their efforts in payload instrument design and construction, and Patti Twigg for her excellent assistance in various aspects of the data analysis. We also appreciate the highly professional efforts of the NASA/Wallops Flight Facility payload team including Charles Manion, Jack Gum, Herb Morgan, Wayne Raemer, and Carl Wipprecht, which led to the success of this program.

REFERENCES

Baker, D. N., P. R. Higbie, R. D. Belian, and E. W. Hones, Jr., Do Jovian electrons influence the terrestrial outer radiation zone?, *Geophys. Res. Lett., 6*, 531, 1979.

Baker, D. N., J. B. Blake, R. W. Klebesadel, and P. R. Higbie, Highly relativistic electrons in the Earth's outer magnetosphere. 1: Lifetimes and temporal history, 1979-1984, *J. Geophys. Res., 91*, 4265, 1986.

Baker, D. N., J. B. Blake, D. J. Gorney, P. R. Higbie, R. W. Klebesadel, and J. H. King, Highly relativistic electrons: A role in coupling to the middle atmosphere, *Geophys. Res. Lett., 14*, 1027, 1987.

Baker, D. N., R. L. McPherron, R. W. Klebesadel, and T. E. Cayton, Linear prediction filter analysis of relativistic electron properties at L = 6.6, *J. Geophys. Res., 95*, 15133, 1990.

Baker, D. N., R. A. Goldberg, F. A. Herrero, J. B. Blake, and L. B. Callis, Satellite and rocket studies of relativistic electrons and their influence on the middle atmosphere, *J. Atmos. Terr. Phys., 54*, 1619, 1993.

De More, W. B., S. P. Sander, D. M. Golden, M.J. Molina, R. F. Hampson, M. J. Kurylo, C. J. Howard, and A. R. Ravishankara, Chemical kinetics and photochemical data for use in stratospheric modeling, *JPL Publication 90-1*, 217 pages, 1990.

Douglass, A. R., C. H. Jackman, and R. S. Stolarski, Comparison of model results transporting the odd nitrogen family with results transporting separate odd nitrogen species, *J. Geophys. Res., 94*, 9862, 1989.

Goldberg, R. A., C. H. Jackman, J. R. Barcus, and F. Sørass, Nighttime auroral energy deposition in the middle atmosphere, *J. Geophys. Res., 89*, 5581, 1984.

Goldberg, R. A., C. L. Croskey, L. C. Hale, J. D. Mitchell, and J. R. Barcus, Electrodynamic response of the middle atmosphere to auroral pulsations, *J. Atmos. Terr. Phys., 52*, 1067, 1990.

Goldberg, R. A., D. N. Baker, F. A. Herrero, S. P. McCarthy, P. A. Twigg, C. L. Croskey, and L. C. Hale, Energy Deposition and Middle Atmosphere Electrodynamic Response to a Highly Relativistic Electron Precipitation Event, *J. Geophys. Res., 98*, In Press, 1994.

Heath, D. F., A. J. Krueger, and P. J. Crutzen, Solar proton event: Influence on stratospheric ozone, *Science, 197*, 886, 1977.

Herrero, F. A., D. N. Baker, and R. A. Goldberg, Rocket measurements of relativistic electrons: New features in fluxes, spectra, and pitch angle distributions, *Geophys. Res. Lett., 18*, 1481, 1991.

Imhof, W. L., H. D. Voss, J. Mobilia, D. W. Datlowe, J. P. McGlennon, and D. N. Baker, Relativistic electron enhancement events: Simultaneous measurements from synchronous and low altitude satellites, *Geophys. Res. Lett., 18*, 397, 1991.

Jackman, C. H., and R. D. McPeters, The response of ozone to solar proton events during solar cycle 21: A theoretical interpretation, *J. Geophys. Res., 90*, 7955, 1985.

Jackman, C. H., and R. D. McPeters, Solar proton events as tests for the fidelity of middle atmospheric models, *Physica Scripta, T18*, 309, 1987.

Jackman, C. H., A. R. Douglass, R. B. Rood, R. D. McPeters, and P. E. Meade, Effect of solar proton events on the middle atmosphere during the past two solar cycles as computed using a two-dimensional model, *J. Geophys. Res., 95*, 7417, 1990.

Jackman, C. H., Effects of energetic particles on minor constituents of the middle atmosphere, *J. Geomag. Geoelectr., 43*, 637, 1991.

Jackman, C. H., A. R. Douglass, K. F. Brueske, and S. A. Klein, The influence of dynamics on two-dimensional model results: Simulations of ^{14}C and stratospheric aircraft NO_X injections, *J. Geophys. Res., 96*, 22559, 1991.

Johnson, R. M., and J. G. Luhmann, Poker Flat MST radar observations of high latitude neutral winds at the mesospause during and after solar proton events, *J. Atmos. Terr. Phys., 55*, 1203, 1993.

McPeters, R. D., and C. H. Jackman, The response of ozone to solar proton events during solar cycle 21: The observations, *J. Geophys. Res., 90*, 7945, 1985.

Nicolet, M., On the production of nitric oxide by cosmic rays in the mesosphere and stratosphere, *Planet. Space Sci., 23*, 637, 1975.

Remsberg, E. E., J. M. Russell, III, and C. Y. Wu, An interim reference model for the variability of the middle atmosphere H_2O vapor distribution, *Handbook for the Middle Atmosphere Program, 31*, 50, 1989.

Solomon, S. D. W. Rusch, J. -C. Gerard, G. C. Reid, and P. J. Crutzen, The effect of particle precipitation events on the neutral and ion chemistry of the middle atmosphere. II. Odd hydrogen, *Planet. Space Sci., 29*, 885, 1981.

Solomon, S., G. C. Reid, D. W. Rusch, and R. J. Thomas, Mesospheric ozone depletion during the solar proton event of July 13, 1982; Part II. Comparison between theory and measurements, *Geophys. Res. Lett., 10*, 257, 1983.

Swider, W., and T. J. Keneshea, Decrease of ozone and atomic oxygen in the lower mesosphere during a PCA event, *Planet. Space Sci., 21*, 1969, 1973.

Thomas, R. J., C. A. Barth, G. J. Rottman, D. W. Rusch, G. H. Mount, G. M. Lawrence, R. W. Sanders, G. E. Thomas, and L. E. Clemens, Mesospheric ozone depletion during the solar proton event of July 13, 1982, Part 1, Measurement, *Geophys. Res. Lett., 10*, 253, 1983.

Thorne, R. M., The importance of energetic particle precipitation on the chemical composition of the middle atmosphere, *Pure Appl. Geophys., 118*, 128, 1980.

Weeks, L. H., R. S. CuiKay, and J. R. Corbin, Ozone measurements in the mesosphere during the solar proton event of November 2, 1969, *J. Atmos. Sci., 29*, 1138, 1972, 1972.

WMO, Scientific assessment of ozone depletion: 1991, World Meteorological Organization, Global Ozone Research and Monitoring Project, *Report No. 25*, Ed. by D. L. Albritton, R. T. Watson, S. Solomon, R. F. Hampson, and F. Ormand, 1992.

R. A. Goldberg, F. A. Herrero, Laboratory for Extraterrestrial Physics, Code 690, NASA/Goddard Space Flight Center, Greenbelt, MD 20771

C. H. Jackman, Laboratory for Atmospheres, Code 916, NASA/Goddard Space Flight Center, Greenbelt, MD 20771

D. N. Baker, now at University of Colorado, Dwayne Physics Bldg., Campus Box 392, Boulder, Co. 80309